

## 类 Salen 和 $\beta$ -二酮稀土配合物的晶体结构和荧光性质

邹晓艳<sup>1,2</sup> 马慧媛<sup>\*,1</sup> 庞海军<sup>1</sup> 张凤鸣<sup>1</sup> 李光明<sup>\*,2</sup>

(<sup>1</sup> 哈尔滨理工大学化学与环境工程学院, 哈尔滨 150080)

(<sup>2</sup> 黑龙江大学化学化工与材料学院, 哈尔滨 150080)

**摘要:** 通过 1,3-苯二胺缩邻香兰素和  $\text{Ln}(\text{acac})_3 \cdot \text{H}_2\text{O}$  ( $\text{Ln}=\text{Ce}, \text{Eu}$ ) 反应, 合成了 2 种双核稀土配合物  $[\text{Ce}_2\text{L}(\text{acac})_4(\text{CH}_3\text{OH})]_2 \cdot 2\text{CH}_2\text{Cl}_2$  (**1**) 和  $[\text{Eu}_2\text{L}(\text{acac})_4(\text{CH}_3\text{OH})]_2 \cdot 2\text{CH}_2\text{Cl}_2$  (**2**)。X 射线单晶衍射分析确定了配合物的晶体结构, 配合物中 2 个稀土离子均为 8 配位, 具有相同的反四棱柱的配位构型。荧光性质研究表明配合物 **2** 显示稀土离子和配体共发光, 主要原因是配体 1,3-苯二胺缩邻香兰素的三线态能级与中心离子  $\text{Eu}(\text{III})$  的三线态能级相匹配。

**关键词:** 1,3-苯二胺缩邻香兰素;  $\beta$ -二酮; 镧系配合物; 配位

中图分类号: O614.33<sup>2</sup>; O614.33<sup>8</sup>

文献标识码: A

文章编号: 1001-4861(2016)09-1647-06

DOI: 10.11862/CJIC.2016.217

## Crystal Structures and Luminescent Properties of Salen-Type and $\beta$ -Diketonate Lanthanide Complexes

ZOU Xiao-Yan<sup>1,2</sup> MA Hui-Yuan<sup>\*,1</sup> PANG Hai-Jun<sup>1</sup> ZHANG Feng-Ming<sup>1</sup> LI Guang-Ming<sup>\*,2</sup>

(<sup>1</sup> College of Chemical and Environmental Engineering, Harbin University of Science and Technology, Harbin 150080, China)

(<sup>2</sup> School of Chemistry and Materials Science, Heilongjiang University, Harbin 150080, China)

**Abstract:** Two dinuclear lanthanide complexes  $[\text{Ln}_2\text{L}(\text{acac})_4(\text{CH}_3\text{OH})]_2 \cdot 2\text{CH}_2\text{Cl}_2$  ( $\text{Ln}=\text{Ce}$  (**1**),  $\text{Eu}$  (**2**)) prepared by salen-type ( $\text{H}_2\text{L}=\text{N},\text{N}'$ -bis(2-oxy-3-methoxybenzylidene)-1,2-phenylenediamine) ligand and  $\text{Ln}(\text{acac})_3 \cdot \text{H}_2\text{O}$  ( $\text{acac}=\text{acetylacetonate}$ ) were structurally characterized. X-ray crystallographic analysis reveals that the two  $\text{Ln}(\text{III})$  ions adopt same coordination environments that octa-coordinated  $\text{Ln}(\text{III})$  atoms form square antiprism geometry. Luminescent analysis reveals the  $\text{Eu}(\text{III})$  ion and ligand-centered co-luminescence for complex **2**, which is attributed to the incomplete energy transfer from the triplet state of  $\text{H}_2\text{L}$  to the resonance energy level of the corresponding  $\text{Eu}(\text{III})$  ion. CCDC: 1482355, **1**; 1449142, **2**.

**Keywords:**  $\text{N},\text{N}'$ -bis(2-oxy-3-methoxybenzylidene)-1,2-phenylenediamine;  $\beta$ -diketonate; lanthanide complexes; coordination

## 0 Introduction

Lanthanide complexes constructed from multidentate ligands are of considerable interest because of their unusual luminescence and magnetism<sup>[1-13]</sup>. The well-known multidentate salen-type ligands are able to stabilize different metals in various coordination

environments although their structures are often influenced by a variety of factors such as radii of lanthanide ions, structures of the ligands and counter ions<sup>[14-19]</sup>. In recent years, it is known that the  $\beta$ -diketonate ligand are perfect sensitizers for  $\text{Ln}(\text{III})$  ion luminescence due to their effective sensitization ability to the metal<sup>[20]</sup>. In view of the recent important

收稿日期: 2016-06-03。收修改稿日期: 2016-08-05。

国家自然科学基金(No.51402092, 21471051, 21071038, 21101045)资助项目。

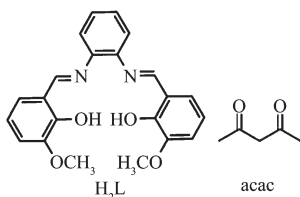
\*通信联系人。E-mail: mahy017@163.com, gmli\_2000@163.com

progress on the structure, luminescence and magnetism of salen-type and  $\beta$ -diketones lanthanide complexes as well as our long-standing research on this domain<sup>[21-25]</sup>, the rigid hexadentate salen-type ligand of *N,N'*-bis(2-oxy-3-methoxybenzylidene)-1,2-phenylenediamine and acetylacetonate were employed to develop salen-type and  $\beta$ -diketonate lanthanide complexes. As a result, two salen-type and  $\beta$ -diketonate dinuclear lanthanide complexes, namely,  $[\text{Ln}_2\text{L}(\text{acac})_4(\text{CH}_3\text{OH})]_2 \cdot 2\text{CH}_2\text{Cl}_2$  ( $\text{Ln}=\text{Ce}$  (**1**),  $\text{Eu}$  (**2**);  $\text{H}_2\text{L}=\text{N,N'}$ -bis(2-oxy-3-methoxybenzylidene)-1,2-phenylenediamine;  $\text{acac}=\text{acetylacetonate}$ ) have been synthesized, and their crystal structures have been determined.

## 1 Experimental

### 1.1 Materials and instruments

All chemicals and solvents except  $\text{Ln}(\text{acac})_3 \cdot \text{H}_2\text{O}$  and  $\text{H}_2\text{L}$  were obtained from commercial sources and used without further purification. The salen-type ligand  $\text{H}_2\text{L}$  (Scheme 1) was prepared according to the literature and lanthanide precursors<sup>[26]</sup>.  $\text{Ln}(\text{acac})_3 \cdot \text{H}_2\text{O}$  were prepared according to a literature procedure previously described<sup>[27]</sup>. Elemental (C, H and N) analyses were performed on a Perkin-Elmer 2400 analyzer. FT-IR data were collected on a Perkin-Elmer 100 spectrophotometer by using KBr disks in the range of 4 000 ~ 500  $\text{cm}^{-1}$ . UV spectra (in methanol) were recorded on a Perkin-Elmer 35 spectrophotometer. Thermal analyses were carried out on a STA-6000 with a heating rate of 10  $^\circ\text{C} \cdot \text{min}^{-1}$  in a temperature range from 30 to 800  $^\circ\text{C}$  in atmosphere. The Powder X-ray diffraction (PXRD) patterns were recorded on a Rigaku D/Max-3B X-ray diffractometer with  $\text{Cu K}\alpha$  radiation ( $\lambda=0.154\ 06\ \text{nm}$ ) under current of 40 mA and voltage of 200 kV, and the scanning rate is 4  $^\circ \cdot \text{s}^{-1}$  with  $2\theta$  ranging from 5  $^\circ$  ~ 40  $^\circ$ .



Scheme 1 Representation of hexadentate salen-type and acac ligand

### 1.2 Synthesis of complexes **1** and **2**

A solution of  $\text{Ln}(\text{acac})_3 \cdot \text{H}_2\text{O}$  ( $\text{Ln}=\text{Ce}$ ,  $\text{Eu}$ ) (1.0 mmol) in  $\text{CH}_3\text{OH}$  (10 mL) were added to a solution of  $\text{H}_2\text{L}$  (0.5 mmol) in  $\text{CH}_2\text{Cl}_2$  (25 mL). The mixed solution was stirred for 4 h at room temperature, and the filtrate was stored in the refrigerator to crystallize at low temperature (278 K). Yellow crystals suitable for single-crystal X-ray diffraction analysis were obtained after 2 days.

$[\text{Ce}_2\text{L}(\text{acac})_4(\text{CH}_3\text{OH})]_2 \cdot \text{CH}_2\text{Cl}_2$  (**1**) Yield: 0.632 g (50.5%); Elemental analysis Calcd. for  $\text{C}_{45}\text{H}_{54}\text{Ce}_2\text{Cl}_4\text{N}_2\text{O}_{13}$ (%): C, 43.14; H, 4.34; N, 2.24; Found(%): C, 43.40; H, 4.20; N, 2.30; IR (KBr,  $\text{cm}^{-1}$ ): 3 431(s), 2 947(w), 1 651(s), 1 645(s), 1 620(s), 1 529(s), 1 476(m), 1 430(m), 1 199(w), 754(w); UV-Vis (MeOH,  $\lambda$ ): 232, 265, 339 nm.

$[\text{Eu}_2\text{L}(\text{acac})_4(\text{CH}_3\text{OH})]_2 \cdot \text{CH}_2\text{Cl}_2$  (**2**) Yield: 0.432 g (73.7%); Elemental analysis Calcd. for  $\text{C}_{45}\text{H}_{54}\text{Eu}_2\text{Cl}_4\text{N}_2\text{O}_{13}$ (%): C, 42.34; H, 4.26; N, 2.19; Found(%): C, 42.40; H, 4.20; N, 2.20; IR (KBr,  $\text{cm}^{-1}$ ): 3 421(s), 2 957(w), 1 654(s), 1 648(s), 1 616(s), 1 521(s), 1 471(m), 1 439(m), 1 198(w), 756(w); UV-Vis (MeOH,  $\lambda$ ): 236, 261, 337 nm.

### 1.3 Crystallography

Single-crystal X-ray data of complexes **1** and **2** were collected on a Rigaku R-AXIS RAPID imaging plate diffractometer with graphite-monochromated  $\text{Mo K}\alpha$  ( $\lambda=0.071\ 073\ \text{nm}$ ) at 293 K. Empirical absorption corrections based on equivalent reflections were applied. The structures of complexes **1** and **2** were solved by direct methods and refined by full-matrix least-squares methods on  $F^2$  using SHELXS-97 crystallographic software package<sup>[28]</sup>. The larger  $U_{\text{eq}}$  values of the dichloromethane molecules might be ascribed to the larger thermal motions of the guest species. All non-hydrogen atoms were anisotropically refined. Selected crystal data and structure refinement details for complexes **1** and **2** were summarized in Table 1.

CCDC: 1482355, **1**; 1449142, **2**.

## 2 Results and discussion

### 2.1 Spectral analysis

Infrared spectra of the ligand, complexes **1** and **2**

**Table 1** Crystal data and structures refinement for complexes **1** and **2**

Complex	<b>1</b>	<b>2</b>
Formula	C <sub>45</sub> H <sub>54</sub> Ce <sub>2</sub> Cl <sub>4</sub> N <sub>2</sub> O <sub>13</sub>	C <sub>45</sub> H <sub>54</sub> Eu <sub>2</sub> Cl <sub>4</sub> N <sub>2</sub> O <sub>13</sub>
Formula weight	1 252.94	1 276.62
Crystal system	Triclinic	Triclinic
Space group	$P\bar{1}$	$P\bar{1}$
<i>a</i> / nm	1.467 0(4)	1.469 4(5)
<i>b</i> / nm	1.598 8(4)	1.604 0(5)
<i>c</i> / nm	2.331 5(7)	2.329 9(5)
$\alpha$ / (°)	101.520(2)	101.517(5)
$\beta$ / (°)	104.172(2)	104.143(5)
$\gamma$ / (°)	91.254(2)	91.298(5)
<i>V</i> / nm <sup>3</sup>	5 180(3)	5 203(3)
<i>Z</i>	4	4
<i>D<sub>c</sub></i> / (g·cm <sup>-3</sup> )	1.606	1.630
$\mu$ / mm <sup>-1</sup>	2.002	2.654
<i>F</i> (000)	2 504	2 544
<i>R</i> <sub>1</sub> [ <i>I</i> >2 $\sigma$ ( <i>I</i> )]	0.065 6	0.052 9
<i>wR</i> <sub>2</sub> [ <i>I</i> >2 $\sigma$ ( <i>I</i> )]	0.169 3	0.123 6
<i>R</i> <sub>1</sub> (all data)	0.087 2	0.072 2
<i>wR</i> <sub>2</sub> (all data)	0.185 1	0.137 7
GOF on <i>F</i> <sup>2</sup>	1.099	1.065

are showed in Fig.S1. In a typical spectrum of complex **1**, the broad weak O-H stretching vibration at 3 414 cm<sup>-1</sup> disappeared, while a weak and broad band at about 3 423 cm<sup>-1</sup> is newly generated from the N-H vibration. The strong  $\nu$ (C=N) bands occurring in the range of 1 647~1 656 cm<sup>-1</sup> for complexes **1** and **2** shifts to higher wavenumber in comparison with that for free H<sub>2</sub>L (1 635 cm<sup>-1</sup>), due to the coordination of C=N groups, which reduces the strengthening of C=N groups. The UV-Vis spectra of the ligand, complexes **1** and **2** are recorded in MeOH solution (Fig.S1 right). For ligand, the typical absorptions at 215, 240 and 309 nm are attributed to the  $\pi$ - $\pi^*$  transition of the aromatic ring and azomethine chromophore. In a typical spectrum of complex **1**, the similar ligand-centered solution absorption bands (236, 261, 337 nm) are observed and red-shifted as compared to those (214, 241 and 310 nm) for ligand resulting from the changes in the energy levels of the ligand orbitals upon the coordination of the Ln(III) ions.

## 2.2 TG-DSC analysis

TG-DSC analysis of complexes **1** and **2** are

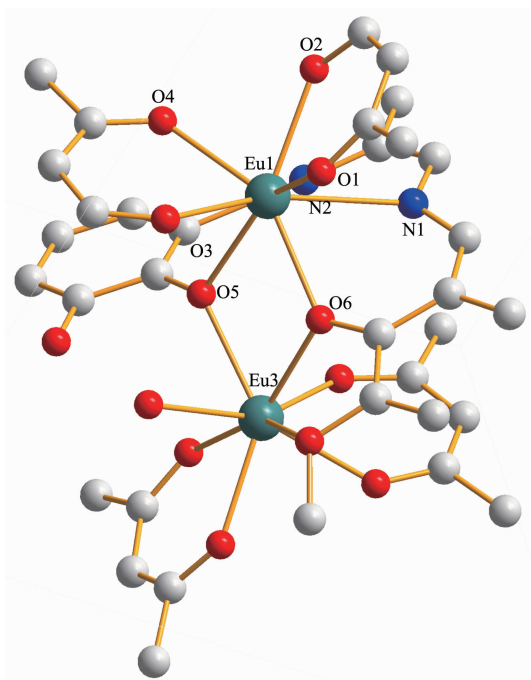
showed in Fig.S2. Complexes **1** and **2** exhibit a gradual weight loss of 11.90% and 12.10% in the range of 33~217 °C, respectively, which corresponds to the loss of two dichloromethane molecules (Calcd. 13.60% and 13.30%, respectively). TG-DSC data confirm that two crystalline dichloromethane exist in complexes **1** and **2**.

## 2.3 PXRD analysis

Powder X-ray diffraction (PXRD) patterns of complexes **1** and **2** are in agreement with the simulated ones (Fig.S3). PXRD analysis further demonstrates that the crystal structure of complexes **1** and **2** is truly representative of the bulk materials. The differences in intensity are due to the preferred orientation of the powder samples.

## 2.4 Structural descriptions of complexes **1** and **2**

X-ray crystallographic analysis reveals that complexes **1** and **2** are isomorphic. In a typical structure of complex **2** shows a dinuclear core structure in which the positive charges of two Eu(III) cations are balanced by one L<sup>2-</sup> and four acac<sup>-</sup>. Complex **2** crystallizes in the triclinic space group  $P\bar{1}$  and as shown in Fig.1,



Hydrogen atoms and solvent molecules are omitted

Fig.1 Molecular structure of complex **2**

complex **2** consists of two types of dinuclear lanthanide clusters. The Eu1(III) ion displays an eight-coordination and is bonded to six oxygen atoms (four from the two top acac ligands and two from the phenolic oxygen of the salen-type ligand) and two nitrogen atoms from the salen-type ligand to form a square antiprism geometry. The Eu3(III) ion displays also an eight-coordination and is bonded to eight oxygen atoms (two oxygen atoms from the phenolic oxygen of the salen-type ligand, four oxygen atoms from the two bottom acac ligands, and two oxygen atom from two methanol molecule) to form a square antiprism geometry as well (Fig.2). The Eu1(III) and

Eu3(III) ions are bridged by the phenolic O5 and O6 atoms forming a rhombus {Eu1O5Eu3O6} core.

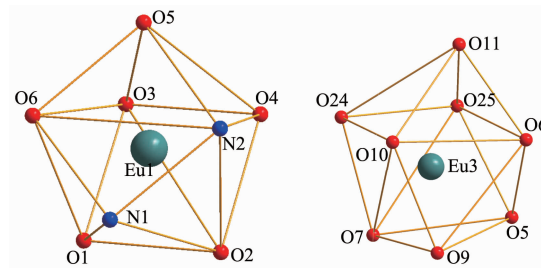


Fig.2 Coordination geometry of Eu(III) ions

## 2.5 Luminescent property

The fluorescence spectrum of complex **2** is recorded in MeOH solution at room temperature (Fig. 3a). The emission spectrum of complex **2** exhibits a weak broad emission band at 450~550 nm with an emission maximum at approximately 510 nm, which can be assigned to the  $\pi-\pi^*$  electronic transition of the ligand. Moreover, the emission spectrum exhibits an intense peak at 614 nm assigned to  $^5D_0 \rightarrow ^7F_2$  transition of the Eu(III) ion<sup>[29]</sup>. The emission spectrum suggests that the ligand can sensitize the luminescence of Eu(III) ion but both the ligand and the Eu(III) ions are co-luminescence in complex **2** (Fig.3a). Furthermore, complex **2** shows bright red emission under UV illumination. The lifetime for complex **2** is found to be 283.22  $\mu\text{s}$ , which is the longest among the salen-type homo-nuclear lanthanide complexes (Fig.3b).

In general, the widely accepted energy transfer mechanism of the luminescence lanthanide complexes is proposed by Crosby<sup>[30]</sup>. In order to make energy transfer effective, the energy-level match between the lowest triplet energy level ( $T_1$ ) of the ligand and the

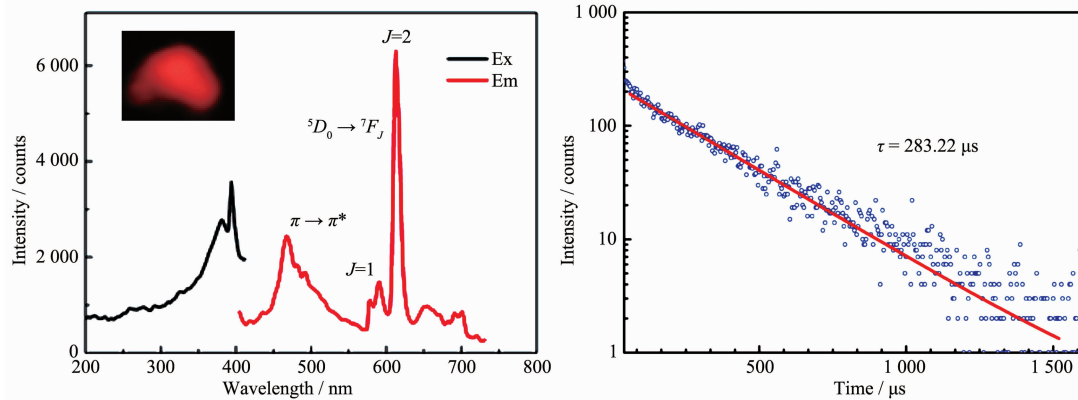


Fig.3 Excitation and emission spectra (a) and experimental luminescence decay profile (b) of complex **2**

lowest excited state level of Ln(III) ion becomes one of the most important factors dominating the luminescence properties of the complexes. On account of the difficulty in observing the phosphorescence spectra of the ligands, the emission spectrum of the complex  $[\text{Gd}_2\text{L}(\text{acac})_4(\text{CH}_3\text{OH})]_4 \cdot 2\text{CH}_2\text{Cl}_2$ <sup>[31]</sup> at 77 K used to estimate the triplet state energy level of the ligand. The single state energy ( $^1\pi\pi^*$ ) level of  $\text{H}_2\text{L}$  is estimated by referencing its absorbance edge, which is  $25\,000\text{ cm}^{-1}$  (400 nm). The triplet ( $T_1$ ) energy level is calculated by referring to the lower wavelength emission peaks of the corresponding phosphorescence spectrum of Gd(III) complex, which is  $21\,505\text{ cm}^{-1}$  (465 nm). It is known that the gap  $\Delta E(T_1-\text{Ln(III)})$  should be intermediate for maximum energy transfer, too big or too small would decrease the efficiency of energy transfer. According to Latva's empirical rule, an optimal ligand-to-metal energy transfer process for Eu(III) needs the energy gap  $\Delta E(^3\pi\pi^* - ^5D_0) > 2\,500\text{ cm}^{-1}$ <sup>[32]</sup>. Therefore, the energy gaps between the triplet state of  $\text{H}_2\text{L}$  and the resonance energy level of Eu(III) are calculated. For complex **2**, the energy gap  $\Delta E$  ( $3\,495\text{ cm}^{-1}$ ) is higher than the value of  $2\,500\text{ cm}^{-1}$  (Fig.4). In conclusion, the effective inter-system crossing and ligand to metal energy transfer processes can be found

in the complex, which demonstrated that the ligand is suitable for sensitizing the Eu(III) ion luminescence.

### 3 Conclusions

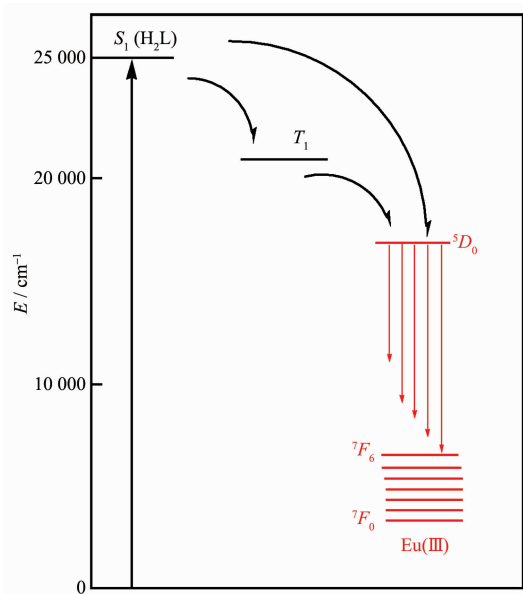
Isolation of complexes **1** and **2** demonstrates that the synthesis of salen-type dinuclear complex with rigid salen-type and  $\beta$ -diketonate ligands are possible, and the structure of the salen-type ligand dominate the structures of the complexes and the coordination geometries of the Ce(III) and Eu(III) ions. The energy gap analysis suggests that the co-luminescence of Eu(III) ion and ligand in complex **2** in MeOH solution is dominated by the good energy match between the triplet state of  $\text{H}_2\text{L}$  and resonance energy level of the corresponding Eu(III) ion. The lifetime for **2** is found to be  $283.22\text{ }\mu\text{s}$ , which is the longest among the salen-type homo-nuclear lanthanide complexes.

**Acknowledgements:** This work is financially supported by the National Natural Science Foundation of China (Grant No. 51402092, 21471051, 21071038 and 21101045).

Supporting information is available at <http://www.wjhxxb.cn>

### References:

- [1] Bogani L, Wernsdorfer W. *Nature*, **2008**,*7*:179-186
- [2] Sorace L, Benelli C, Gatteschi D. *Chem. Soc. Rev.*, **2011**,*40*: 3092-3104
- [3] Woodruff D N, Winpenny R E, Layfield R A. *Chem. Rev.*, **2013**,*113*:5110-5148
- [4] Yamanouchi M, Chiba D, Matsukura F. *Nature*, **2004**,*428*: 539-542
- [5] Liu T Q, Yan P F, Luan F, et al. *Inorg. Chem.*, **2015**,*54*:221-228
- [6] Ishikawa N, Sugita M, Ishikawa T, et al. *J. Am. Chem. Soc.*, **2003**,*125*:8694-8695
- [7] Zhao L, Wu J, Ke H, et al. *CrystEngComm*, **2013**,*15*:5301-5309
- [8] AlDamen M A, Clemente J M, Coronado E. *J. Am. Chem. Soc.*, **2008**,*130*:8874-8875
- [9] AlDamen M A, Cardona S, Clemente J M. *Inorg. Chem.*, **2009**,*48*:3467-3479
- [10] Guo Y N, Chen X H, Xue S. *Inorg. Chem.*, **2011**,*50*:9705-9713



$S_1$ : first excited singlet state;  $T_1$ : first excited triplet state

Fig.4 Schematic energy level diagram and energy transfer processes for complex **2**

- [11]Liu J, Chen Y C, Liu J L, et al. *J. Am. Chem. Soc.*, **2016**, **138**:5441-5450
- [12]Chen Y C, Liu J L, Ungur L, et al. *J. Am. Chem. Soc.*, **2016**, **138**:2829-2837
- [13]ZOU Xiao-Yan(邹晓艳), YAN Peng-Fei(闫鹏飞), ZHANG Feng-Ming(张凤鸣), et al. *Chinese J. Inorg. Chem.*(无机化学学报), **2013**, **29**(8):1680-1686
- [14]Jiang S D, Wang B W, Su G A. *Angew. Chem. Int. Ed.*, **2010**, **49**:7448-7451
- [15]Long J, Habib F, Lin P H, et al. *J. Am. Chem. Soc.*, **2011**, **133**: 5319-5328
- [16]Zou H H, Wang R Z, Chen L, et al. *Dalton Trans.*, **2014**, **43**: 2581-2587
- [17]Zou X Y, Yan P F, Dong Y P, et al. *RSC Adv.*, **2015**, **5**: 96573-96579
- [18]Yue Y M, Yan P F, Sun J W, et al. *Polyhedron*, **2015**, **94**: 90-95
- [19]Chien Y L, Chang M W, Tsai Y C, et al. *Polyhedron*, **2015**, **102**:8-15
- [20]Zucchi G, Murugesan V, Tondelier D, et al. *Inorg. Chem.*, **2011**, **50**:4851-4856
- [21]Li B, Li H F, Chen P, et al. *Phys. Chem. Chem. Phys.*, **2015**, **17**:30510-30517
- [22]Zhang J W, Li H F, Chen P, et al. *J. Mater. Chem. C*, **2015**, **3**:1799-1806
- [23]Leng J Q, Li H F, Chen P, et al. *Dalton Trans.*, **2014**, **43**: 12228-12235
- [24]Lin P H, Sun W B, Yu M F, et al. *Chem. Commun.*, **2011**, **47**: 10993-10995
- [25]Sun W B, Han B L, Lin, P H, et al. *Dalton Trans.*, **2013**, **42**: 13397-13403
- [26]Koner R, Lee G H, Wang Y, et al. *Eur. J. Inorg. Chem.*, **2005**, **8**:1500-1505
- [27]Stites J G, McCarty C, Quill L L. *J. Am. Chem. Soc.*, **1948**, **70**: 3142-3143
- [28]Sheldrick G M. *Acta Crystallogr., Sect. A*, **2007**, **64**:112-122
- [29]Zhang H J, Gou R H, Yan L, et al. *Spectrochim. Acta Part A*, **2007**, **66**:289-294
- [30]Crosby G R, Whan R E, Alire R M. *J. Chem. Phys.*, **1961**, **34**:743
- [31]ZOU Xiao-Yan(邹晓艳), YAN Peng-Fei(闫鹏飞), DONG Yan-Ping(董艳萍), et al. *J. Eng. Heilongjiang Univ.*(黑龙江大学工程学报), **2015**, **6**(4): 27-31
- [32]Latva M, Takalo H, Mikkala V M, et al. *J. Lumin.*, **1997**, **75**: 149-169